tvst

https://doi.org/10.1167/tvst.8.3.31

Article

Histopathologic Assessment of Optic Nerves and Retina From a Patient With Chronically Implanted Argus II Retinal Prosthesis System

Tai-Chi Lin[1–4,*], Lei-Chi Wang[1,5,6,*], Lan Yue[1,2], Yi Zhang[1], Paulo Falabella[1,7], Danhong Zhu[1,8], David R. Hinton[1,8], Narsing A. Rao[1,8], David G. Birch[9], Rand Spencer[10], Jessy D. Dorn[11], and Mark S. Humayun[1,2]

[1] Department of Ophthalmology, USC Roski Eye Institute, University of Southern California, Los Angeles, CA, USA
[2] USC Ginsburg Institute for Biomedical Therapeutics, University of Southern California, Los Angeles, CA, USA
[3] Department of Ophthalmology, Taipei Veterans General Hospital, Taipei, Taiwan, Republic of China
[4] Institute of Clinical Medicine, National Yang-Ming University, Taipei, Taiwan, Republic of China
[5] Department of Pathology and Laboratory Medicine, Taipei Veterans General Hospital, Taipei, Taiwan, Republic of China
[6] School of Medicine, National Yang-Ming University, Taipei, Taiwan, Republic of China
[7] Department of Ophthalmology and Visual Sciences, Federal University of São Paulo, São Paulo, Brazil
[8] Department of Pathology, Keck School of Medicine, University of Southern California, Los Angeles, CA, USA
[9] Retina Foundation of the Southwest, Dallas, TX, USA
[10] Texas Retina Associates, Dallas, TX, USA
[11] Second Sight Medical Products, Inc., Sylmar, CA, USA

Correspondence: Mark S. Humayun, USC Ginsburg Institute for Biomedical Therapeutics, 1450 San Pablo Street, Room 6545B, Los Angeles, CA 90033, USA. e-mail: humayun@usc.edu

Received: 3 December 2018
Accepted: 1 April 2019
Published: 30 May 2019

Keywords: histopathology; retinal prosthesis; retinitis pigmentosa

Citation: Lin T-C, Wang L-C, Yue L, Zhang Y, Falabella P, Zhu D, Hinton DR, Rao NA, Birch DG, Spencer R, Dorn JD, Humayun MS. Histopathologic assessment of optic nerves and retina from a patient with chronically implanted Argus II retinal prosthesis system. Trans Vis Sci Tech. 2019;8(3):31, https://doi.org/10.1167/tvst.8.3.31

Purpose: To characterize histologic changes in the optic nerve and the retina of an end-stage retinitis pigmentosa (RP) patient after long-term implantation with the Argus II retinal prosthesis system.

Methods: Serial cross sections from the patient's both eyes were collected postmortem 6 years after implantation. Optic nerve from both eyes were morphometrically analyzed and compared. Retina underneath and outside the array was analyzed and compared with corresponding regions in the fellow eye.

Results: Although the optic nerve of the implant eye demonstrated significantly more overall atrophy than the fellow eye ($P < 0.01$), the temporal quadrant that retinotopically corresponded to the location of the array did not show additional damage. The total neuron count of the macular area was not significantly different between the two eyes, but the tack locations and their adjacent areas showed significantly fewer neurons than other perimacular areas. There was an increased expression of glial fibrillary acidic protein (GFAP) throughout the retina in the implant eye versus the fellow eye, but there was no significant difference in the cellular retinaldehyde-binding protein (CRALBP) expression. Except for the revision tack site, no significant increase of inflammatory reaction was detected in the implant eye.

Conclusion: Long-term implantation and electrical stimulation with an Argus II retinal prosthesis system did not result in significant tissue damage that could be detected by a morphometric analysis.

Translational Relevance: This study supports the long-term safety of the Argus II device and encourages further development of bioelectronics devices at the retina-machine interface.

Introduction

Bioelectronic retinal implants that bypass the photoreceptor layer and directly stimulate the inner retinal neurons have been shown to restore useful vision in patients who have been blinded for decades by outer retinal degenerative diseases.[1–3] The Argus II retinal prosthesis system (Second Sight Medical Products, Inc., Sylmar, CA) is an epiretinal implant that contains an array of 6×10 electrodes surgically attached to the inner surface of retina, nearby the ganglion cell layer. It received European Union (CE Mark) approval in 2011 and United States Food and Drug Administration (FDA) market approval in 2013.

The entire system includes multiple external and internal parts. The images captured by a miniature glasses–mounted camera is delivered to an external video processing unit (VPU) worn by the user for pixilation and processing. The processed information is relayed to the external transceiver coil that is built into the side arm of the glasses, from where the visual information and the power is wirelessly transmitted to the implant. The extraocular components of the implant, an internal transceiver coil and a metal case enclosed Application-Specific-Integrated-Circuit (ASIC) chip, recover the radio frequency signals and generate electrical pulses that are delivered via a transscleral cable to the intraocular electrode array, roughly stimulating a visual angle of $11° \times 19°$.

The surgical procedure of Argus II implantation includes a 360° limbal conjunctival peritomy and placement of an encircling scleral band, which secures the hermetic electronics enclosure and the episcleral transceiver coil. After performing pars plana vitrectomy, including shaving of the vitreous base to allow insertion of the electrode array without vitreous traction, the electrode array is inserted and racked to the retina. The extraocular portion of the cable is anchored to the sclera with suture.

Between 2007 and 2009, a total of 30 participants received the Argus II implant in the United States and Europe.[4,5] The 5-year results published in 2016 indicate that Argus II continues to function and reliably enables basic visual functions in these patients.[6] Previous studies on long-term implantation and electrical stimulation of Argus I, a 16-electrode first generation epiretinal implant preceding Argus II, supported its long-term use and did not reveal damages either in the optic nerve or in the retina.[7,8] In comparison with Argus I, the Argus II array contains a higher electrode density that covers a larger retinal area to increase the spatial resolution and meanwhile accommodate a greater visual field. Therefore, it is not clear whether surgical implantation of Argus II and chronic electrical stimulation from its array will have an impact on the health of the optic nerve and retina. Among the 30 implanted subjects in the Argus II trial, one subject died from natural causes 6 years after implantation. Histology of her eyes provides a unique opportunity to assess the histopathologic alterations in the optic nerve and retina after Argus II implantation. Hereby, we present a morphometric analysis of the subject's eyes, further deciphering the long-term biosafety of Argus II and similar epiretinal prostheses.

Methods

Study Subject

The study patient, at death, was a 77-year-old Caucasian woman with an ocular history of retinitis pigmentosa (RP) and extracapsular cataract extraction. The subject provided informed consent to participate in an FDA-approved Investigational Device Exemption study with approval from the institutional review board of the University of Southern California. The research complied with the Declaration of Helsinki. The patient was implanted with the Argus II retinal prosthesis system in the right eye for the Argus II feasibility study (http://clinicaltrials.gov/show/NCT00407602) in 2008. Her visual acuity (VA) was bare light perception in both eyes due to profound RP. The surgical implantation, electrical stimulation parameters, and array characteristics were described in detail elsewhere.[4,5] There were no adverse events reported after implantation, but the patient received an elective revision surgery that moved the array to a more foveal location and added a second tack for improved apposition to the retina. The array remained fixed over the macula until the patient's death from natural causes approximately 6 years after implantation.

Tissue Processing

The eyes were harvested by Lions Eye Bank with their standard protocol and the length of time from death to fixation was less than 24 hours. Two globes with attached optic nerve were fixed in 4% formaldehyde solution. The retrobulbar optic nerve within 1 mm from the globe was dissected into cross sections to minimize disruption of the retinotopic order in the

Table. Antibodies Used for Immunohistochemical Staining

Antibodies	Clone and Dilution
NF	Clone N52.1.7, 1:50; Leica (Vista, CA)
NSE	Clone 22C9, 1:200; Leica
GFAP	Clone GA5, 1:400; Leica
CD68	Clone 514H12, 1:100; Leica
CD31	Clone 1A10, 1:50; Leica
CRALBP	Clone B2 (ab15051), 1:5000; Abcam (Burlingame, CA)
Rhodopsin	Clone RET-P1, 1:400; Abcam
RPE-65*	Polyclonal, 1:500; Abcam

* RPE-65 was used for immunofluorescence assay.

myelinated fibers. The cross sections were processed, embedded in paraffin, and serially sectioned at 5-μm intervals for further processing and analysis of the optic nerve. The formalin-fixed globes, including the macular region where the array was implanted, were sectioned horizontally (nasal-temporal). The pupil-optic nerve (P-O) sections of each eye were embedded in paraffin and serially sectioned at 5-μm intervals for further processing and analysis of the retina.

Staining of the Optic Nerve

Cross sections of the optic nerve of both eyes were stained with hematoxylin and eosin (H&E) at 50-μm intervals. Three selected sections of each optic nerve were stained with neurofilament (NF) to identify axons within.

Staining of the Globe

P-O sections of each globe were stained with H&E at 50-μm intervals for morphometric analysis. The H&E staining delineates landmarks, such as optic nerve head and macula (implantation site of the array), for immunohistochemical staining of the selected slides. Neurons of the retina were identified with the neuron specific enolase (NSE) staining. Glial fibrillary acidic protein (GFAP) staining was used to highlight the astrocytes as well as the active Müller cells. An antibody against cellular retinaldehyde-binding protein (CRALBP), a Müller cell marker, was used to identify both quiescent and active Müller cells.[9,10] Photoreceptor cells were identified with Rhodopsin staining. To evaluate foreign body reaction surrounding the implant, CD68 and H&E staining were used to reveal the macrophages and multinucleated giant cells, respectively. The retinal pigmented epithelial (RPE) cells were identified with an RPE-65 antibody. The antibodies used are listed in the Table.

Morphometric Analysis of the Optic Nerve

Three NF-stained sections of each optic nerve were selected, analyzed, and computed for the mean axon densities. The optic nerve quadrants were designated as superior, inferior, nasal, and temporal based on the landmarks established before separation of the optic nerve from the globe. NF immunoreactivity was quantified based on the microscopic images (Olympus BX53 microscope, field diameter 0.55 mm and Olympus DP 27 camera; Olympus, Center Valley, PA) that were acquired at the ×400 magnification. Images of each optic nerve quadrant were imported into the ImageJ software (National Institute of Health, Bethesda, MD) for analysis. Adjustment of color threshold was performed to distinguish between areas of immunoreactivity and background. Mean axon densities within each optic nerve quadrant were computed as the ratio of immunoreactive area to the total area. Kruskal-Wallis test was performed to determine the statistical significance of the difference in the mean axon densities between the implant versus fellow eye as well as among different optic nerve quadrants.

Morphometric Analysis of the Retina

Macular and perimacular regions in contact with the epiretinal array were analyzed. The retina underneath the array was divided into 16 equivalent regions in a 4×4 grid (Fig. 1). NSE-stained sections were photographed at a magnification of ×400 for manual counting. The neurons were counted by nuclei. Total neuron counts were calculated in each of the 16 regions covering the macular and perimacular area. Each region contained four cross sections from which the neurons were counted. As a control, the macular area of the left eye (fellow eye) was divided into four equivalent regions. Kruskal-Wallis test was performed to determine the statistical significance of the difference in the neuron counts between the macular area of two eyes and among each region of the implant eye.

To evaluate the expression of GFAP, CRALBP, and CD68 in the retina of both eyes, the following locations in the implant eye were sampled: the macular region underneath the array, peripheral regions without the array, and the tack sites. For

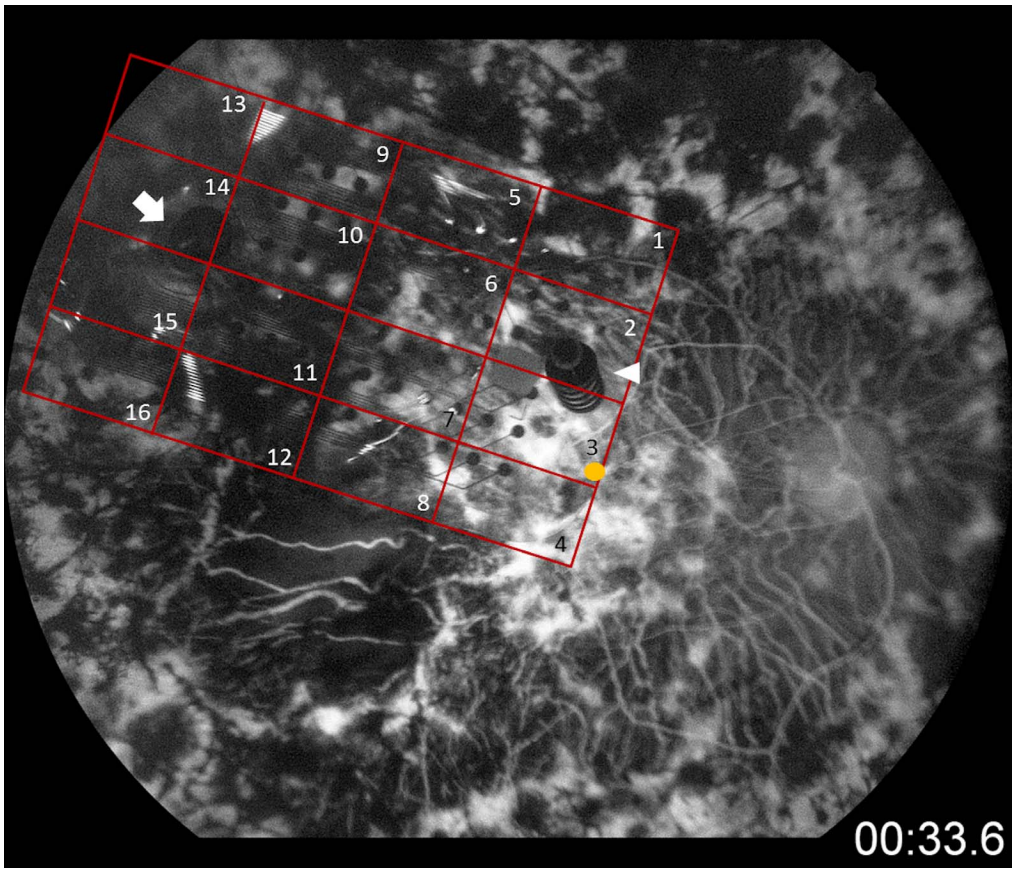

Figure 1. Fluorescein angiography of the implant eye. The retina underneath the array was divided into 16 equivalent regions in a 4 × 4 grid for analysis. *Yellow circle*: foveola. *White arrow*: original tack. *White triangle*: revision tack.

comparison, the corresponding locations of the fellow eye were also sampled. All images of GFAP and CRALBP stained sections were acquired at the ×400 magnification. The immunoreactivity of GFAP and CRALBP were quantified using the same method as NF. The number of CD68-positive cells was counted manually from digital images collected at ×200. Kruskal-Wallis test was performed for statistical analysis. All data are presented in the form of average ± standard deviation.

Results

Surgical implantation of the Argus II enabled the subject to perform in visual function tests and functional vision assessments with better results while using the device.[4,5] For the first 12 months, the subject had low-detection thresholds at most electrodes and the device enabled her to detect direction of motion of moving objects. Possibly limited by the age, the subject's mobility was not measurably better with the device on. The subject reported detecting the outline of trees, a dog, and ripples on a lake. Toward the end of the first year her thresholds rose substantially, and the optical coherence tomography (OCT) scans showed a substantial gap between the device and the retina. The decision was made to perform revision surgery, with a second tack through the heel of the electrode array. While anatomically successful, the functional outcome was poor and the number of functional electrodes remained low. Nevertheless, she continued to use the device as instructed for 1 to 1.5 hr/d although it did not help her much. She did not use the system outside. It was extremely difficult to perform ophthalmic imaging for the patient, because of her age, inability to fixate, and eye movements. Due to advanced RP, the segmentation of the retinal nerve fiber layer (NFL) is tenuous at best. As revealed by the OCT images, the NFL of the right eye was slightly thinner than that of the left eye before implantation and not much change in the NFL was found in the right eye over 6 years of device activity (Fig. 2). The patient died 6 years post implantation from natural causes and the eyes were

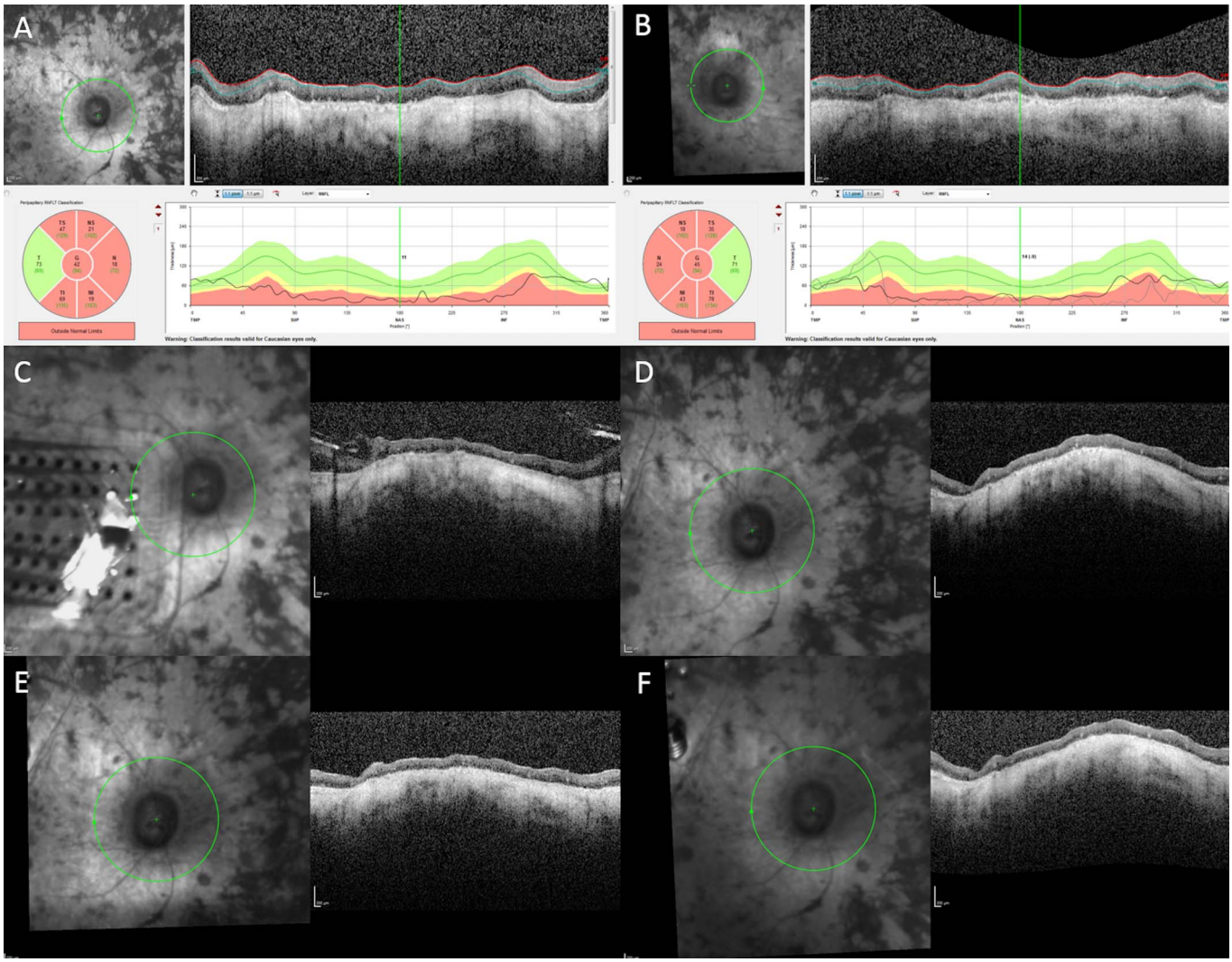

Figure 2. OCT images of the retinal NFL of the right eye (A) and the left eye (B) before implantation. NFL of right eye 1 year after implantation (C). NFL of right eye 1 (D), 2 years (E), and three years (F) after revision surgery.

collected postmortem to characterize the histologic features secondary to the epiretinal array implantation and chronic electrical stimulation. The eyes were harvested and fixed in formalin within 24 hours after death. Two globes with optic nerve attached were fixed adequately where no postmortem changes, such as ischemic necrosis of the cells, were found with thorough examination of all the slides. Optic nerve of the implant eye exhibited significant atrophy in comparison with that of the fellow eye (Fig. 3). The mean axon density was 4.79 ± 2.06 in the implant eye optic nerve, significantly less than 13.27 ± 6.43 in the fellow eye ($P < 0.001$). Axon density was also separately analyzed in each optic nerve quadrant. The temporal quadrant of the implant eye optic nerve corresponded to the perimacular region where the epiretinal array was implanted and electrical stimulation applied. This quadrant did not appear to show more damage in comparison with the other quadrants of the same optic nerve (Fig. 4).

The total neuron count in the macular area was 156 ± 102 in the implant eye and 212 ± 56 in the fellow eye. Kruskal-Wallis test did not show a significant difference ($P = 0.105$; Figs. 4A, 4B). Comparison between each of the 16 perimacular regions indicated a significant reduction in the neuron count in the regions nearby the tack, where a fibrotic membrane was formed (Figs. 5C, 5D, and 6). Examination of multiple sections around the tack insertion site and its adjacent areas revealed consistent features of fibrotic membrane formation with loss of neurons. The fibrotic tissue was labeled by

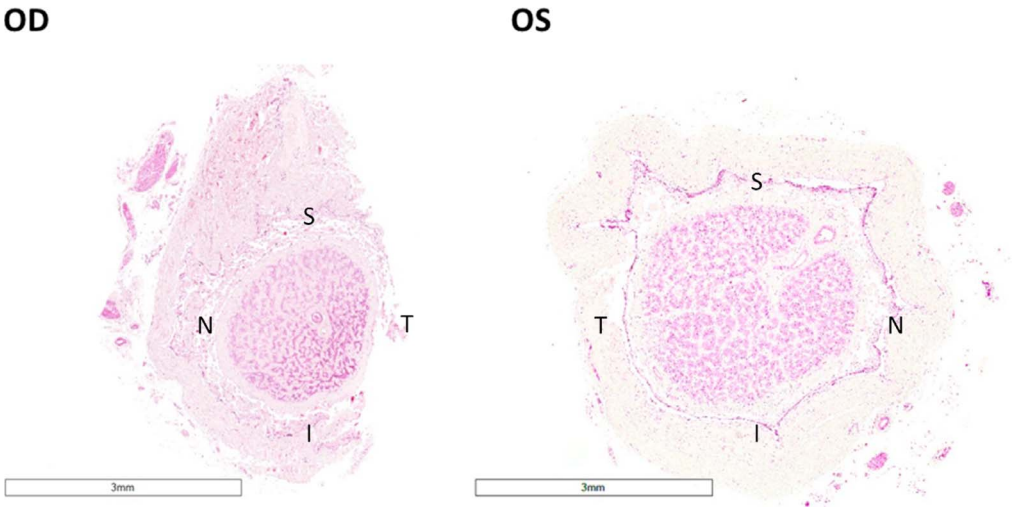

Figure 3. H&E staining of the patient's optic nerve in the implant eye (OD) and the fellow eye (OS). Optic nerve of the implant eye showed significant atrophy, as evidenced by the decrease in diameter. (×1, acquired by Aperio digital pathology system) S, superior; T, temporal; I, inferior; N, nasal.

Masson's Trichrome staining that highlights the dense composition of collagen deposition (Fig. 5F).

There was an upregulation of GFAP expression throughout the entire retina in both eyes. The average density of GFAP expression was 55.22 ± 10.94 in the perimacular region of the implant eye and 28.50 ± 5.33 in the corresponding region of the fellow eye ($P < 0.001$). There was no significant difference in CRALBP expression across different regions of both eyes. For example, in the implant eye, the average density of CRALBP expression was 26.78 ± 11.66 in the right macular region, 28.68 ± 4.38 in the left macular region ($P = 0.157$ between right and left macular region), 22.69 ± 5.16 in the right peripheral region ($P = 0.432$ between right macular and peripheral region), and 28.30 ± 4.98 in the left peripheral region ($P = 0.347$ between right and left peripheral region).

Except for the area where the revision tack was placed, the retina underneath the array exhibited no significant increase in the average count of CD68-positive macrophages in comparison with the corresponding regions of the fellow eye (Fig. 7). No remaining photoreceptor cells were identified throughout both retinas with Rhodopsin staining, consistent with the end-stage RP in both eyes.

Discussion

Our group has previously performed a morphometric analysis of the eyes of an end-stage RP patient implanted with the Argus I array, finding no damage in the optic nerve and the retina.[7] Given the significant difference in electrode density and stimulation area between the Argus I and II arrays, the present study sought to characterize the impact of Argus II implantation on the optic nerve and retina.

The optic nerve of the implant eye showed significant atrophy in comparison with the fellow eye.[7] Atrophy is apparent by the increased presence of the connective tissues between nerve fascicles, the decreased number of axons, and the reduced overall diameter of the optic nerve (Figs. 3, 4). Atrophic appearance of the optic nerve head is a funduscopic hallmark of the RP patients, but the histopathology of the optic nerve has not been well studied.[11] A study of 14 RP eyes obtained from autopsy revealed little, if any, atrophy in the early stage, but significant atrophy in the advanced stage of the disease.[12] Since the Argus II implantation was performed in the subject's worse-seeing eye,[4] it was not surprising to find exacerbated atrophy in the implant eye. Electrophysiologic activity of the optic nerve could provide a better understanding of the optic atrophy in the implanted eye over time. However, visual-evoked potential (VEP) examination is not a routine clinical evaluation for Argus II implanted patients.[4] Therefore, we suggest a protocol for all actual implanted patients to include a VEP examination before and every year after the implantation.

A study of 35 postmortem human eyes found a rough retinotopic order within the optic nerve immediately posterior to the globe, in which the foveal fibers occupied a large portion of the temporal

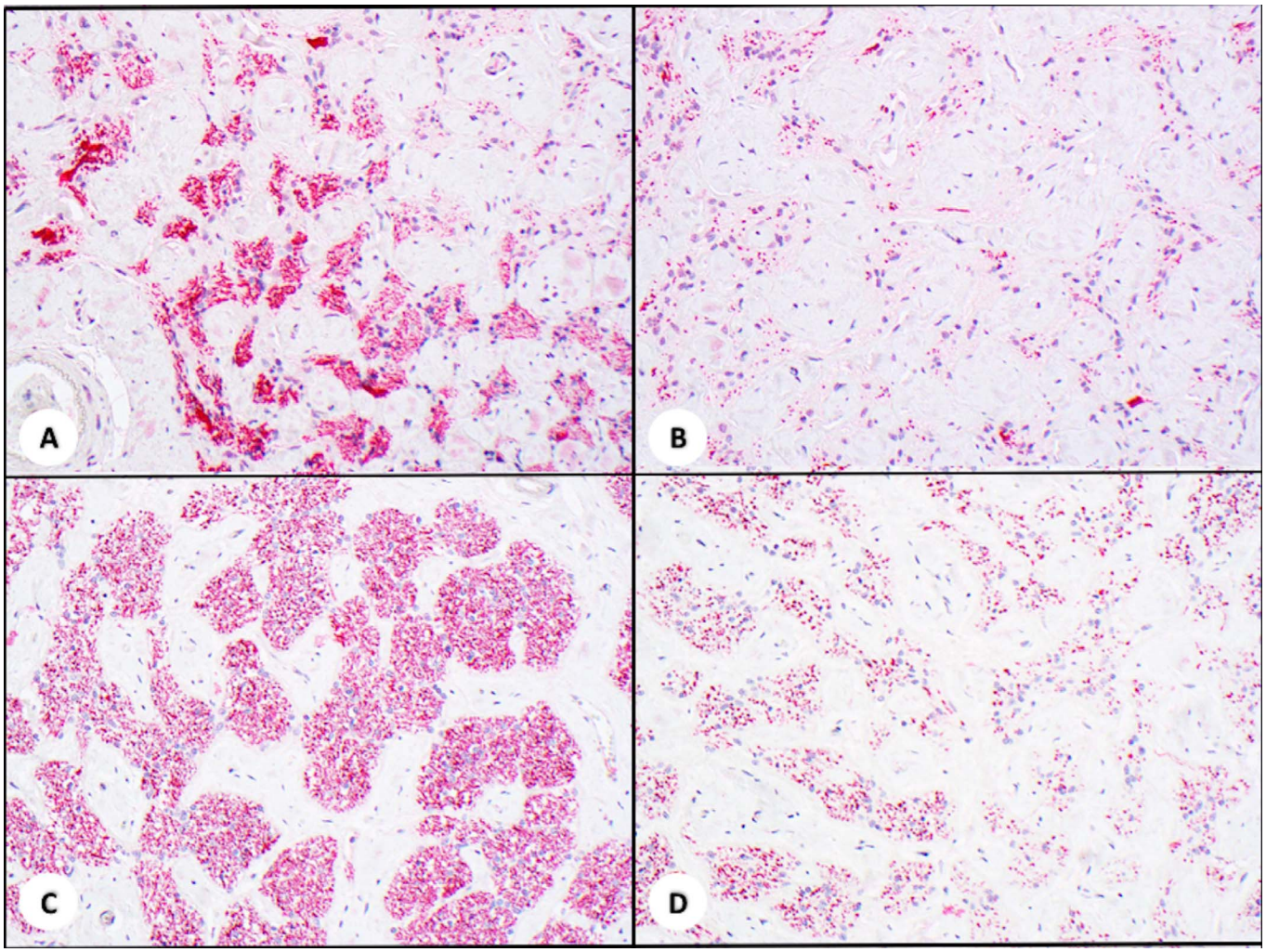

Figure 4. NF staining of the optic nerves in the right eye temporal quadrant (A), right eye nasal quadrant (B), left eye temporal quadrant (C), and left eye nasal quadrant (D) (×200). The mean axon density was lower in the implant eye (right eye) compared with the fellow eye ($P < 0.001$). The temporal quadrant of the implant eye optic nerve, retinotopically corresponding to the retinal area underneath the array, did not show additional damage than the nasal quadrant of the right eye.

side of the optic nerve.[13] As such, the temporal quadrant of the implant eye optic nerve is considered to correspond to the retinal region where the array was implanted and stimulation delivered.[7] Despite an overall, more notable atrophy in the optic nerve in the implant eye, the temporal quadrant did not exhibit more damage than other quadrants, similar to previous findings with the Argus I[7] (Fig. 4). This suggested that the histologic changes in the optic nerve secondary to the epiretinal array implantation may not result from electrical stimulation of the retina but rather transneuronal degeneration,[12,14] because otherwise the optic nerve in the temporal quadrant would have shown more atrophy than the others quadrants. Nevertheless, some of the limitations regarding the evaluation of optic nerve axon atrophy in the implanted eye are worth noting. For example, total axon counts can be highly dependent on the counting technique,[7] and large variations in axon counts may occur between normal optic nerves even when controlling for age.[15,16] Therefore, in the future cases, it would be better for the eyes to be fixed in glutaraldehyde solution, which is ideal for electron microscopy analysis. Electron microscopy can provide additional information of degenerated myelin which reflects the severity of axon atrophy.

The initial degenerative changes in RP eyes occur in the photoreceptors. In advanced stages, extensive degeneration or loss of photoreceptors was found throughout the retina.[11,12] The present study with the Rhodopsin staining revealed no remaining rods and the fact that the subject had bare light perception

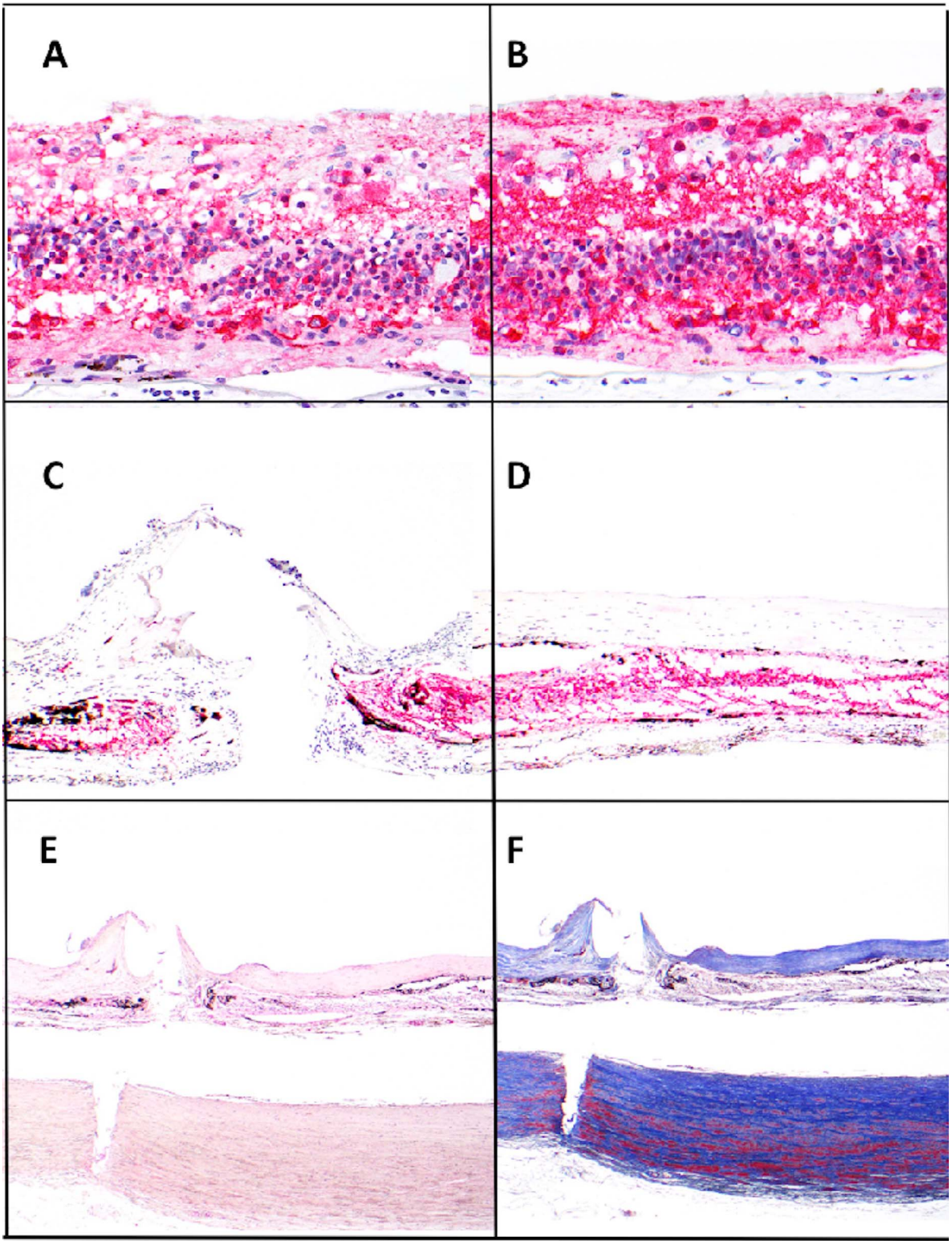

Figure 5. Sections of retina from implanted and fellow eyes. Consistent highly remodeled retina was found across all sections. Retinal neuron counts were calculated from NSE staining (A–D) and tack penetration shown by H&E and Masson Trichrome staining (E, F). The total neuron counts of the macular area showed no significant difference between both eyes. ([A] implant eye, [B] fellow eye, NSE, ×400). Significant loss of neurons was only revealed at and near the tack with fibrosis formation ([C] tack site, [D] adjacent areas with fibrotic →

←
membrane, NSE, ×100). Deposition of dense collagen in the fibrotic membrane was readily identified with H&E and Masson Trichrome stain. The tack sites showed an all layer penetrated wound from the retina through the choroid, and to the outer lamina of the sclera ([E] H&E, ×40, [F] Masson Trichrome, ×40).

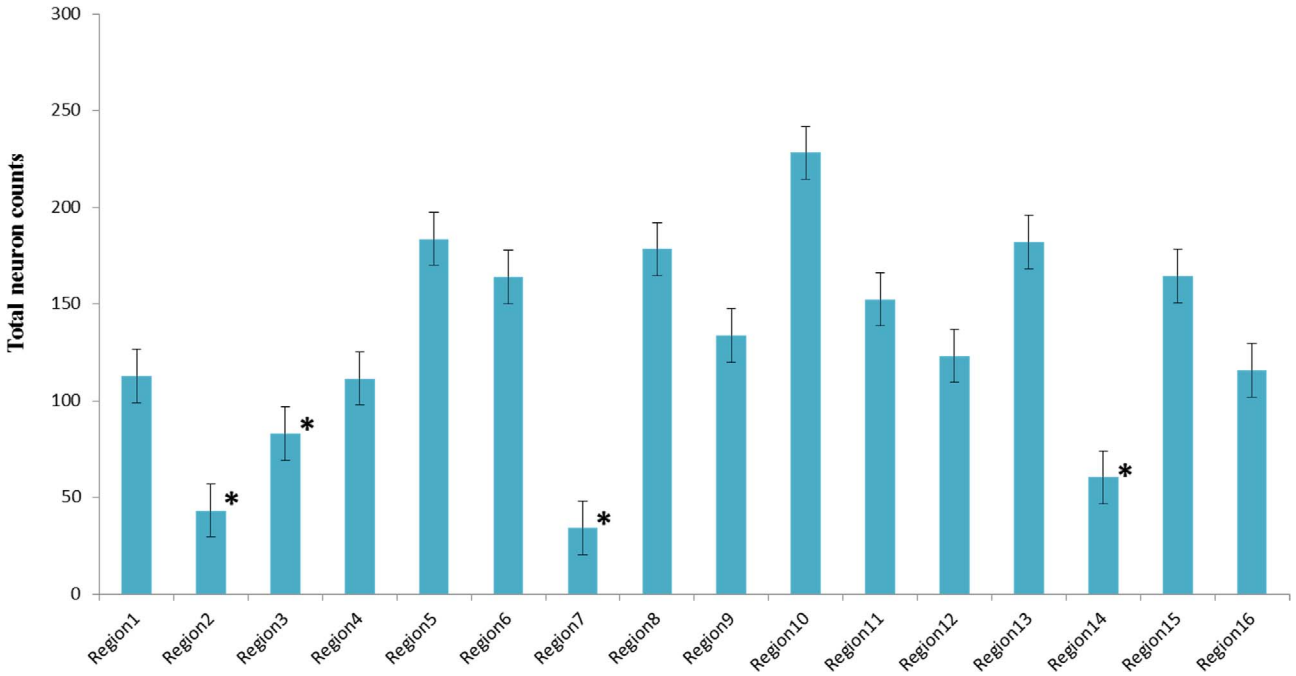

Figure 6. Neuron counts of the 16 perimacular regions underlying the epiretinal array. Significant reduction of neuron counts was found at and nearby the location of the tracks, along with formation of fibrosis.

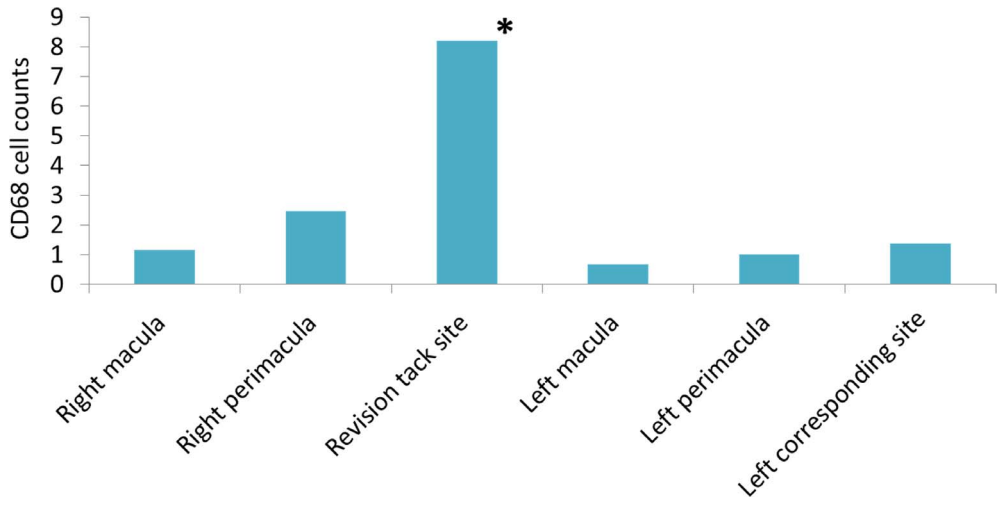

Figure 7. The average counts of CD68-positive macrophages of the retina underlying the array, and the corresponding regions of the fellow eye.

suggests little if any survival of cones, consistent with the subject's end-stage RP status. It has been previously reported that in advanced RP despite near-total loss of the photoreceptors, approximately 80% of the inner nuclear layer and 30% of the ganglion cell layer survived in the macular region.[17] Due to significant reorganization of the remaining inner retina, counting neurons from each cellular layer is challenging in end-stage RP eyes. Therefore, in the present study, we counted the total number of neurons without differentiating the contribution from each cellular layer. The results did not show a significant difference in the neuron count in the macular area between the implant versus the fellow eye, but markedly fewer neurons were found specifically nearby the tack sites, where the formation of a fibrotic membrane was observed. Histologic changes in the vicinity of a retinal tack, such as fibrosis formation,[7] scarring,[18] and loss of retinal layers,[19] have been described elsewhere. The implant eye under our investigation had two tacks to fix the array to the retina. The tacks penetrated through all layers of the retina and into the sclera. Intraocular fibrosis proliferation as seen in penetrating injuries[20,21] developed around the tacks during the healing of the insertion wounds. The fibroblasts produced large amount of collagen that was deposited in the regions adjacent to the tack sites.[22] The reduction in cell count was observed in the fibrosis proliferated retinal areas only, but not in the other areas covered by the array, which suggests that the cell loss was likely to arise from tack-caused tissue injuries, rather than proximity to the array.

Reactive gliosis, characterized by the upregulation of GFAP expression,[23–26] is a feature of many neurodegenerative diseases of the retina, including RP.[11] Müller cells are one of the major contributors of gliosis in the retina in the early stage of degeneration.[25,26] In end-stage RP, astrocytes undergo reactive hyperplasia in the inner retina after loss of the retinal ganglion cells, also contributing to gliosis.[11] A study of 21 postmortem eyes with RP showed up to a 70% loss of total retinal ganglion cells in severe cases, in comparison with normal eyes.[17] Previous animal studies have demonstrated that reactive astrocytes proliferated after brain injury[27,28] and reactive astrocytes distant from the lesion originated from hypertrophy while those close to the lesion arise from hyperplasia of the glial cells.[27] In our study, increase of GFAP immunoreactivity was found throughout the retina in both eyes, indicating that the reactive astrocytic gliosis occurred likely due to loss of retinal ganglion cells in end-stage RP. Further, our results showed that the increase of GFAP immunoreactivity in the perimacular region of the implant eye was significantly higher than that of the fellow eye, which may reflect astrocytic hyperplasia around the tacks and astrocytes hypertrophy in the adjacent regions.

In an animal study, Müller cells were demonstrated to be sensitive to mechanical stress perpendicularly to the retinal surface, mediating mechanically induced changes in the retinal architecture.[29] Our results show no significant difference in CRALBP expression between the implant and the fellow eye, revealing minimal, if any, damage from the pressure applied by the array against the retina.

Except for the revision tack site, there was no significant increase in the number of CD68-positive histiocytes and giant cells in the implant eye. Furthermore, RPE65 staining revealed that the intraretinal pigmented cells were RPE cells, which migrated into the neural retina following photoreceptor degeneration.[11,12,30] Overall, these findings demonstrate that the implanted array did not induce an active inflammatory reaction.

In conclusion, the eyes collected postmortem from the Argus II patient 6 years after implantation provide a unique opportunity for a morphometric analysis of the retina and the optic nerve after chronic electrical stimulation. The results show that axonal damage in the optic nerve and neuronal loss in the retina of the implant eye was likely due to the end-stage RP and the injury from tack insertion. Despite the higher number of electrodes and larger retinal area associated with the Argus II array than the Argus I array, there was no evidence of additional tissue damage at the nontack area, regardless of the electrical stimulation or the pressure. As such, this original study provides histologic evidence that supports the long-term safety of the Argus II device and it encourages further development of bioelectronics devices at the retina-machine interface. However, this study is not designed to rule out possibility of subtle subcellular changes. The number of subjects who have been implanted and that have deceased is very small therefore a greater case number to further support our conclusions is not available, which may pose a limitation to the study.

Acknowledgments

Supported by grants from the USC Ginsburg Institute for Biomedical Therapeutics, University of Southern California, Los Angeles, California, United

States, and an unrestricted grant to the USC Department of Ophthalmology from Research to Prevent Blindness, New York, NY.

Disclosure: **T.-C. Lin**, None; **L.-C. Wang**, None; **L. Yue**, None; **Y. Zhang**, None; **P. Falabella**, None; **D. Zhu**, None; **D.R. Hinton**, None; **N.A. Rao**, None; **D.G. Birch**, None; **R. Spencer**, None; **J.D. Dorn**, Second Sight Medical Products (E,P); **M.S. Humayun**, Second Sight Medical Products (F, I, C) P

*T-CL and L-CW contributed equally to this manuscript.

References

1. Humayun MS, de Juan E Jr, Dagnelie G, Greenberg RJ, Propst RH, Phillips DH. Visual perception elicited by electrical stimulation of retina in blind humans. *Arch Ophthalmol*. 1996; 114:40–46.
2. Margalit E, Maia M, Weiland JD, et al. Retinal prosthesis for the blind. *Surv Ophthalmol*. 2002; 47:335–356.
3. Yanai D, Weiland JD, Mahadevappa M, Greenberg RJ, Fine I, Humayun MS. Visual performance using a retinal prosthesis in three subjects with retinitis pigmentosa. *Am J Ophthalmol*. 2007; 143:820–827.
4. Humayun MS, Dorn JD, da Cruz L, et al. Interim results from the international trial of Second Sight's visual prosthesis. *Ophthalmology*. 2012; 119:779–788.
5. Ho AC, Humayun MS, Dorn JD, et al. Long-term results from an epiretinal prosthesis to restore sight to the blind. *Ophthalmology*. 2015; 122:1547–1554.
6. da Cruz L, Dorn JD, Humayun MS, et al. Five-year safety and performance results from the Argus II retinal prosthesis system clinical trial. *Ophthalmology*. 2016;123:2248–2254.
7. Eng JG, Agrawal RN, Tozer KR, et al. Morphometric analysis of optic nerves and retina from an end-stage retinitis pigmentosa patient with an implanted active epiretinal array. *Invest Ophthalmol Vis Sci*. 2011;52:4610–4616.
8. Yue L, Falabella P, Christopher P, et al. Ten-year follow-up of a blind patient chronically implanted with epiretinal prosthesis Argus I. *Ophthalmol*. 2015;122:2545–2552.e2541.
9. Bu SC, Kuijer R, van der Worp RJ, et al. Immunohistochemical evaluation of idiopathic epiretinal membranes and in vitro studies on the effect of TGF-beta on Müller cells. *Invest Ophthalmol Vis Sci*. 2015;56:6506–6514.
10. Wahlin KJ, Campochiaro PA, Zack DJ, Adler R. Neurotrophic factors cause activation of intracellular signaling pathways in Müller cells and other cells of the inner retina, but not photoreceptors. *Invest Ophthalmol Vis Sci*. 2000;41:927–936.
11. Milam AH, Li ZY, Fariss RN. Histopathology of the human retina in retinitis pigmentosa. *Prog Retin Eye Res*. 1998;17:175–205.
12. Gartner S, Henkind P. Pathology of retinitis pigmentosa. *Ophthalmology*. 1982;89:1425–1432.
13. Fitzgibbon T, Taylor SF. Retinotopy of the human retinal nerve fibre layer and optic nerve head. *J Comp Neurol*. 1996;375:238–251.
14. Stone JL, Barlow WE, Humayun MS, de Juan E, Jr., Milam AH. Morphometric analysis of macular photoreceptors and ganglion cells in retinas with retinitis pigmentosa. *Arch Ophthalmol*. 1992; 110:1634–1639.
15. Mikelberg FS, Yidegiligne HM, Schulzer M. Optic nerve axon count and axon diameter in patients with ocular hypertension and normal visual fields. *Ophthalmology*. 1995;102:342–348.
16. Repka MX, Quigley HA. The effect of age on normal human optic nerve fiber number and diameter. *Ophthalmology*. 1989;96:26–32.
17. Santos A, Humayun MS, de Juan E Jr, et al. Preservation of the inner retina in retinitis pigmentosa. A morphometric analysis. *Arch Ophthalmol*. 1997;115:511–515.
18. Walter P, Szurman P, Vobig M, et al. Successful long-term implantation of electrically inactive epiretinal microelectrode arrays in rabbits. *Retina*. 1999;19:546–552.
19. Majji AB, Humayun MS, Weiland JD, Suzuki S, D'Anna SA, de Juan E Jr. Long-term histological and electrophysiological results of an inactive epiretinal electrode array implantation in dogs. *Invest Ophthalmol Vis Sci*. 1999;40:2073–2081.
20. Topping TM, Abrams GW, Machemer R. Experimental double-perforating injury of the posterior segment in rabbit eyes: the natural history of intraocular proliferation. *Arch Ophthalmol*. 1979;97:735–742.
21. Cleary PE, Ryan SJ. Histology of wound, vitreous, and retina in experimental posterior penetrating eye injury in the rhesus monkey. *Am J Ophthalmol*. 1979;88:221–231.
22. Mutsaers SE, Bishop JE, McGrouther G, Laurent GJ. Mechanisms of tissue repair: from wound healing to fibrosis. *Int J Biochem Cell Biol*. 1997;29:5–17.

23. Chua J, Nivison-Smith L, Fletcher EL, Trenholm S, Awatramani GB, Kalloniatis M. Early remodeling of Müller cells in the rd/rd mouse model of retinal dystrophy. *J Comp Neurol*. 2013;521:2439–2453.
24. Roche SL, Ruiz-Lopez AM, Moloney JN, Byrne AM, Cotter TG. Microglial-induced Müller cell gliosis is attenuated by progesterone in a mouse model of retinitis pigmentosa. *Glia*. 2018;66:295–310.
25. Ekstrom P, Sanyal S, Narfstrom K, Chader GJ, van Veen T. Accumulation of glial fibrillary acidic protein in Müller radial glia during retinal degeneration. *Invest Ophthalmol Vis Sci*. 1988;29:1363–1371.
26. Felmy F, Pannicke T, Richt JA, Reichenbach A, Guenther E. Electrophysiological properties of rat retinal Müller (glial) cells in postnatally developing and in pathologically altered retinae. *Glia*. 2001;34:190–199.
27. Schiffer D, Giordana MT, Cavalla P, Vigliani MC, Attanasio A. Immunohistochemistry of glial reaction after injury in the rat: double stainings and markers of cell proliferation. *Int J Dev Neurosci*. 1993;11:269–280.
28. Mathewson AJ, Berry M. Observations on the astrocyte response to a cerebral stab wound in adult rats. *Brain Res*. 1985;327:61–69.
29. Lindqvist N, Liu Q, Zajadacz J, Franze K, Reichenbach A. Retinal glial (Müller) cells: sensing and responding to tissue stretch. *Invest Ophthalmol Vis Sci*. 2010;51:1683–1690.
30. Hartong DT, Berson EL, Dryja TP. Retinitis pigmentosa. *Lancet*. 2006;368:1795–1809.